Supporting Information

for

Ruthenium(II) N–Heterocyclic Carbene Polymer Based Sensors for Detection of Predatory Drugs like Ketamine and Scopolamine

Nupoor Gopal Neole[a,b], Zhoveta Yhobu[a], Jan Grzegorz Małecki[c], Doddahalli H. Nagaraju[d], and Srinivasa Budagumpi*[a]

[a] *Centre for Nano and Material Sciences, Jain University, Jain Global Campus, Kanakapura, Ramanagaram, Bangalore 562112, India*

[b] *Department of Forensic Science, School of Sciences, JAIN (Deemed–to–be University), J. C. road, Sudhama Nagar, Bangalore-560027, Karnataka, India*

[c] *Institute of Chemistry, University of Silesia, 9th Szkolna St., 40–006 Katowice, Poland*

[d] *Department of Chemistry, School of Applied Sciences, REVA University, Kattigenahalli, Yelahanka, Bangalore 560064, India*

* Corresponding author:

E–mail: b.srinivasa@jainuniversity.ac.in (Dr. S. Budagumpi)

Table SI1. Crystal data and structure refinement parameters for salt ruthenium NHC organometallic polymer **6**.

Empirical formula	$C_{20}H_{18}Br_2N_{10}Ru_2$
Formula weight	760.4
Crystal system	monoclinic
Space group	Cc
a/Å	21.2545(14)
b/Å	15.6065(9)
c/Å	7.4968(4)
α/°	90
β/°	90.204(5)
γ/°	90
Volume/Å^3	2486.7(3)
Z	4
ρ_{calc}g/cm^3	2.031
μ/mm^{-1}	4.458
F(000)	1464
Crystal size/mm^3	0.27 × 0.14 × 0.03
Radiation	Mo Kα (λ = 0.71073)
2Θ range for data collection/°	7.538 to 58.766
Index ranges	-26 ≤ h ≤ 29, -18 ≤ k ≤ 21, -9 ≤ l ≤ 10
Reflections collected	10829

Table SI2. Important bond distances and angles of ruthenium NHC organometallic polymer **6.**

Module	**Angle/°**	**Module**	**Length /A°**
Br1-Ru1-Br11	81.42(4)	Ru1-Br11	2.908(2)
Br2-Ru1-Br1	95.27(7)	Ru1-Br11	2.866(2)
Br2-Ru1-Br11	104.24(7)	Ru1-Br2	2.569(2)
C1-Ru1-Br11	102.2(4)	Ru1-C1	2.107(14)
C1-Ru1-Br1	114.4(4)	Ru2-Br1	2.563(3)
C1-Ru1-Br2	142.7(4)	Ru2-Br2	2.854(3)
Br1-Ru2-Br2	95.72(7)	Ru2-C11	2.149(17)
C11-Ru2-Br1	148.1(5)	N1-N2	1.359(18)
C11-Ru2-Br2	116.1(5)	N1-C1	1.343(19)
Ru1-Br1-Ru12	139.77(10)	N1-C8	1.47(2)
Ru2-Br1-Ru12	72.97(7)	N2-C2	1.29(2)
Ru2-Br1-Ru1	71.42(7)	N3-C1	1.385(19)
Ru1-Br2-Ru2	71.54(6)	N3-C2	1.39(2)
N2-N1-C8	117.8(13)	N3-C3	1.43(2)
C1-N1-N2	117.3(13)	N4-C3	1.32(2)
C1-N1-C8	125.0(13)	N4-C7	1.34(3)
C2-N2-N1	103.3(13)	N5-C10	1.12(3)
C1-N3-C2	110.1(13)	N6-N7	1.36(2)
C1-N3-C3	126.5(12)	N6-C11	1.26(2)
C2-N3-C3	123.5(13)	N6-C18	1.45(2)
C3-N4-C7	116.0(16)	N7-C12	1.28(2)
N7-N6-C18	119.5(14)	N8-C11	1.39(2)
C11-N6-N7	115.5(14)	N8-C12	1.39(2)
C11-N6-C18	125.0(16)	N8-C13	1.42(2)
C12-N7-N6	104.0(15)	N9-C13	1.32(2)
C11-N8-C13	130.8(15)	N9-C17	1.32(3)
C12-N8-C11	106.1(14)	N10-C20	1.15(2)
C12-N8-C13	122.9(13)	C3-C4	1.39(2)
C13-N9-C17	115.2(18)	C4-C5	1.34(3)
N1-C1-Ru1	125.2(10)	C5-C6	1.36(3)
N1-C1-N3	99.2(12)	C6-C7	1.34(3)
N3-C1-Ru1	135.4(10)	C8-C9	1.51(3)
N2-C2-N3	110.1(14)	C9-C10	1.48(3)
N4-C3-N3	112.6(14)	C13-C14	1.41(3)
N4-C3-C4	124.3(16)	C14-C15	1.35(3)
C4-C3-N3	123.1(15)	C15-C16	1.39(3)
C5-C4-C3	117.2(17)	C16-C17	1.36(3)
C4-C5-C6	119.9(19)	C18-C19	1.51(2)
C7-C6-C5	119.7(19)	C19-C20	1.49(2)

Table SI3. Comparative data for detection of predatory drugs with different techniques in current and past work.

Drugs	*Technique*	*LOD*	*Matrix*	*Reference*
Ketamine	KT-MIM/MOFs@G/SPE with DPV	4.0×10^{-11} mol/L	PBS buffer	[1]
	PAMAM-CDs (Electrochemiluminescence)	0.067 ng/ mL	PBS buffer	[2]
	G4HTD/PtNPs/CPE with DPV	1.0×10^{-7} mol/L	Briton buffer	[3]
	GCMS	0.01 g/mL	Britton –Robinson buffer, urine and plasma	[4]
	Ru(II)NHC+MWCNTs/ GCE with SWV	0.194 nM (0.0531 µg/L)	Britton –Robinson buffer, alcoholic and non-alcoholic beverages	This work
Scopolamine	GSH–Co_3O_4/GCE with DPV	0.001 µM	Britton –Robinson buffer and urine	[5]
	SDBS/MWCNTs - CPE with DPV	0.449 ng/mL	PBS buffer, D. stramonium seeds, leaves and eye drops	[6]
	SPE with CV	3.9 µM	Phosphate buffer, coca cola	[7]
	Activated 3D-graphene with SWV	1 µM	Britton –Robinson buffer, vodka, white wine, whiskey, energy drink	[8]
	Ru(II)NHC+MWCNTs/ GCE with SWV	3.81 nM (1.669 µg/L)	Britton –Robinson buffer, beer, artificial serum	This work

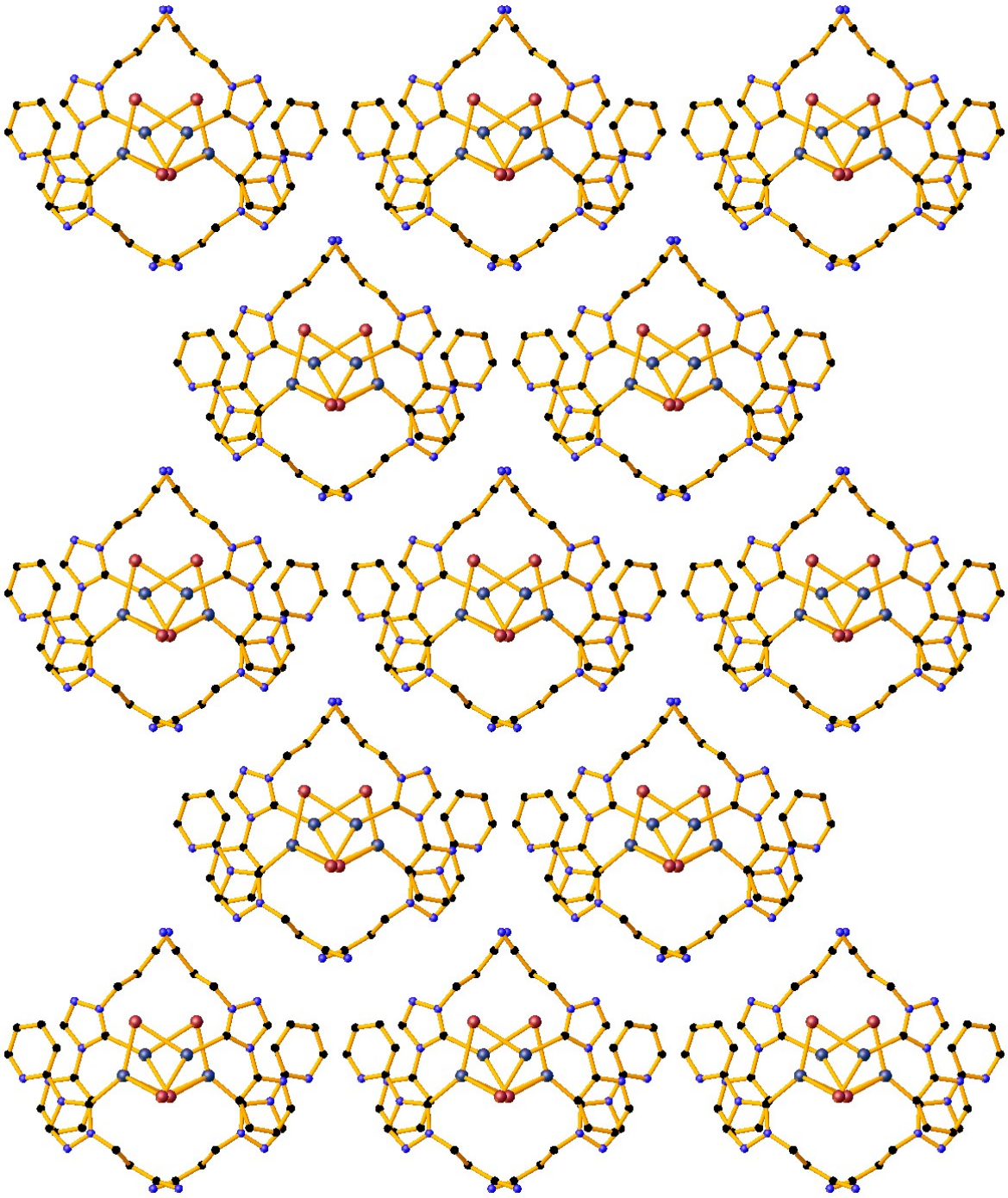

Figure SI1: Crystal packing image of ruthenium organometallic polymer **6**. Hydrogen atoms are omitted for clarity.

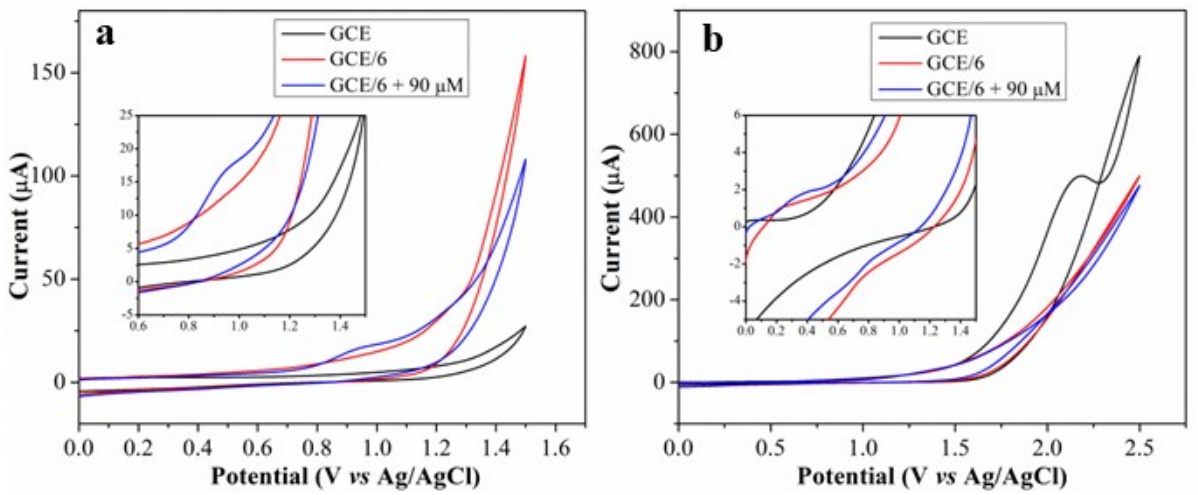

Figure SI2: CV study of GCE and ruthenium organometallic polymer **6** for 90 µM **(a)** ketamine and **(b)** scopolamine.

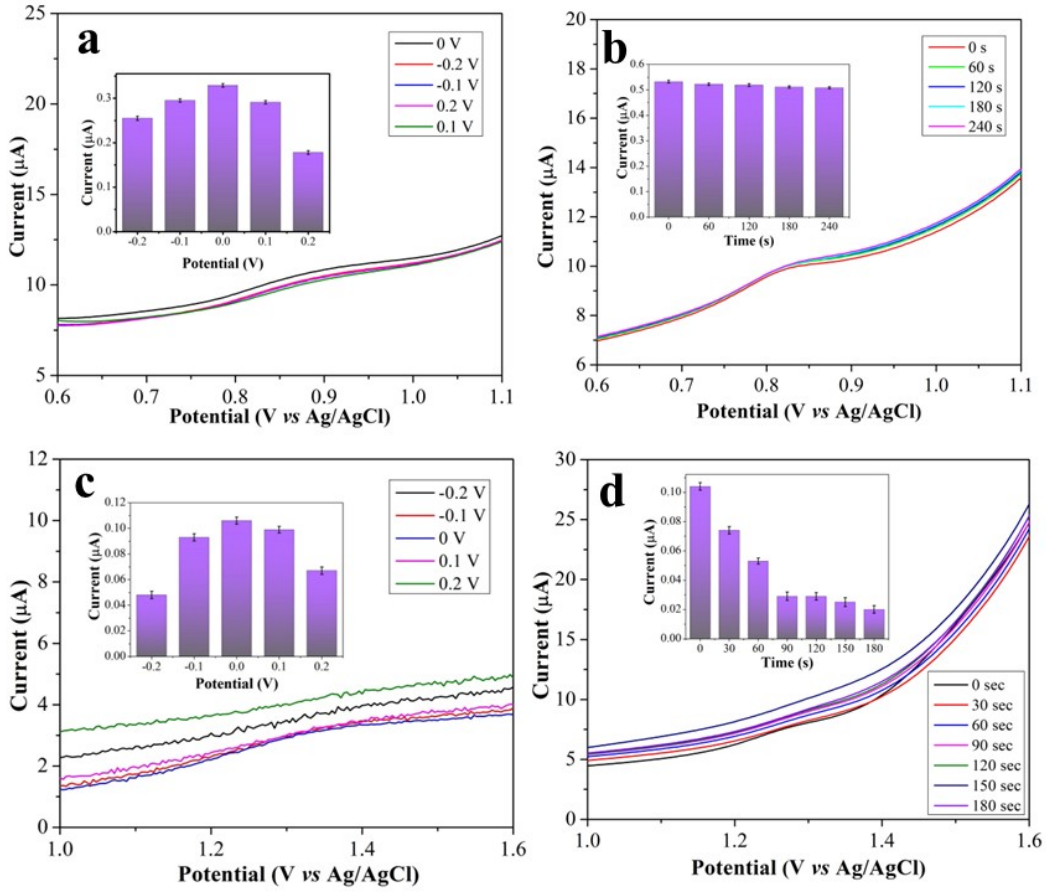

Figure SI3: Optimisation with complex **6** modified GCE with 30 µM ketamine (a) accumulation potential (b) accumulation time and with 50 µM scopolamine (c) accumulation potential, (d) accumulation time.

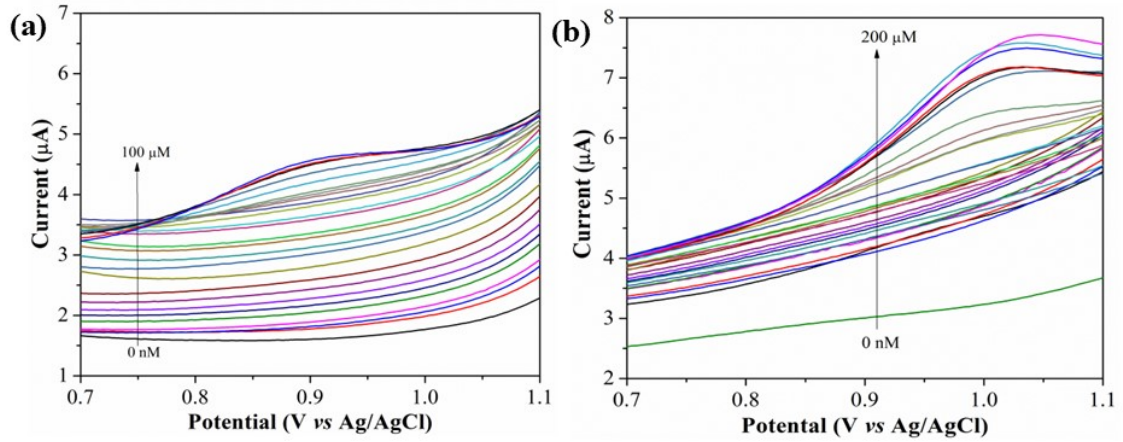

Figure SI4: Concentration dependent SWV responses of **6** modified GCE (a) and **7** modified GCE (b) towards ketamine quantification in Britton–Robinson buffer of pH 8 at room temperature.

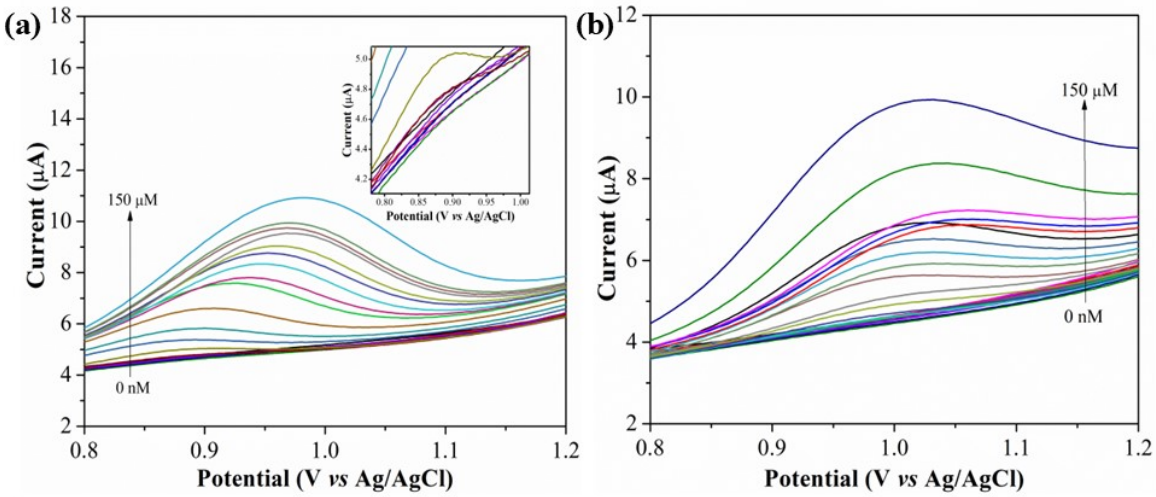

Figure SI5: Concentration dependent SWV responses of **6** modified GCE (a) and **7** modified GCE (b) towards scopolamine quantification in Britton–Robinson buffer of pH 7 at room temperature.

NMR spectra

The following figures represent the NMR spectra of salts and their corresponding ruthenium NHC organometallic polymers [9].

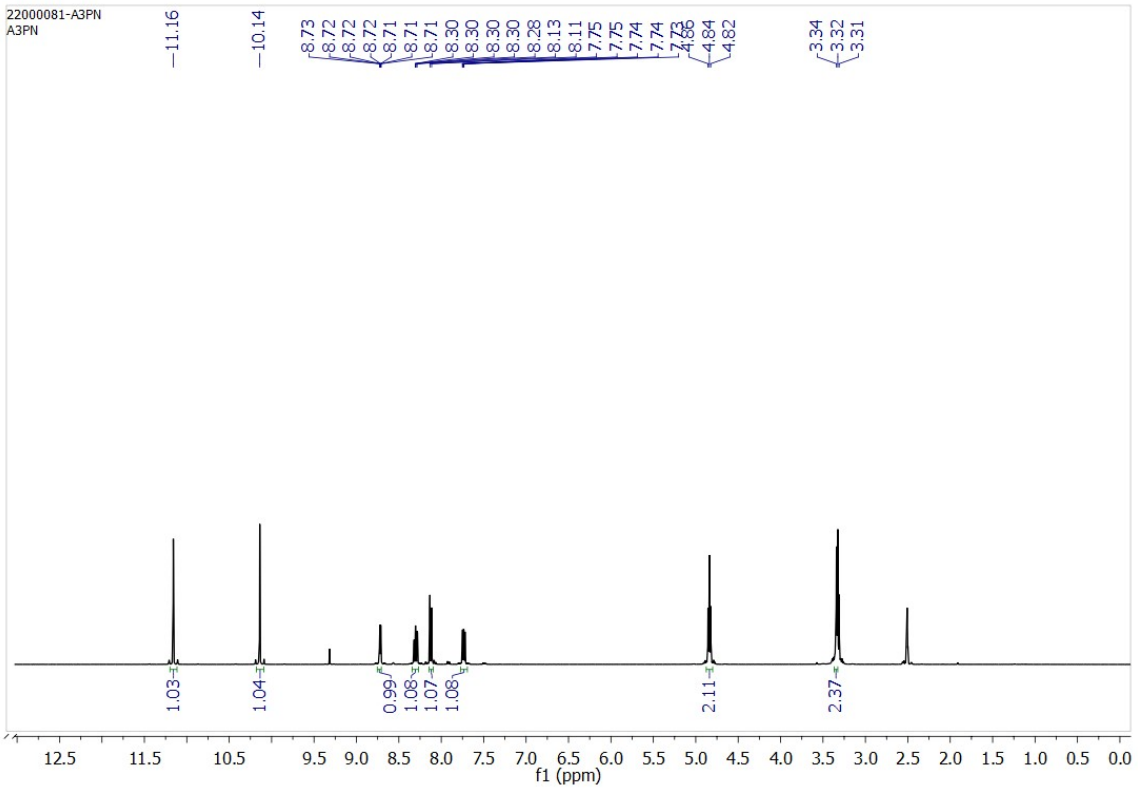

Figure SI6: ^{1}H−NMR spectrum of salt **4** in d_6-DMSO at room temperature.

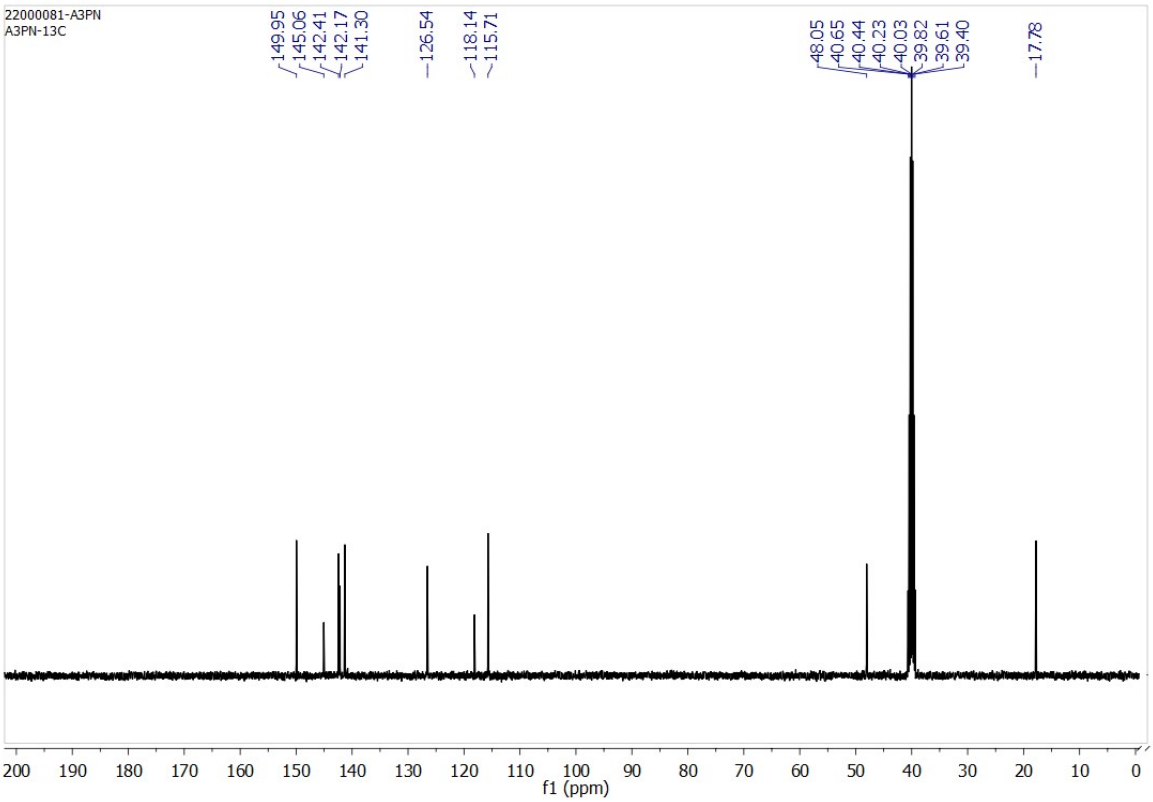

Figure SI7: ^{13}C−NMR spectrum of **4** in d_6-DMSO at room temperature.

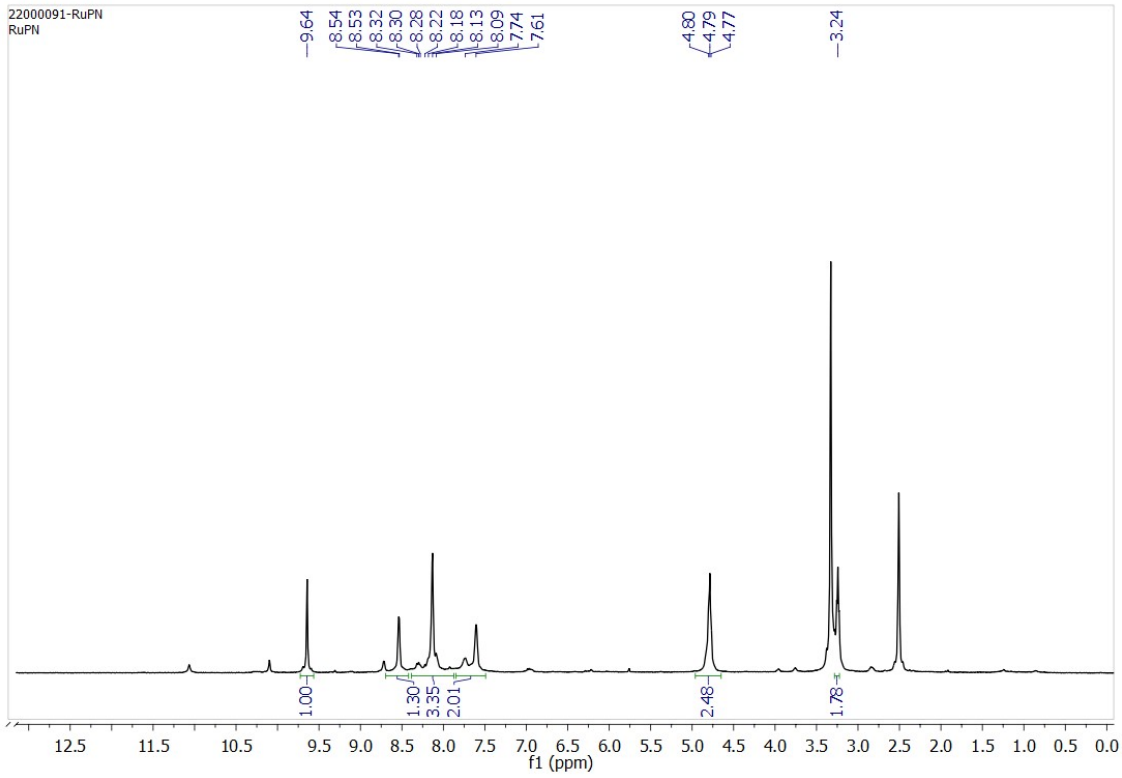

Figure SI8: ^{1}H−NMR spectrum of **6** in d_6-DMSO at room temperature.

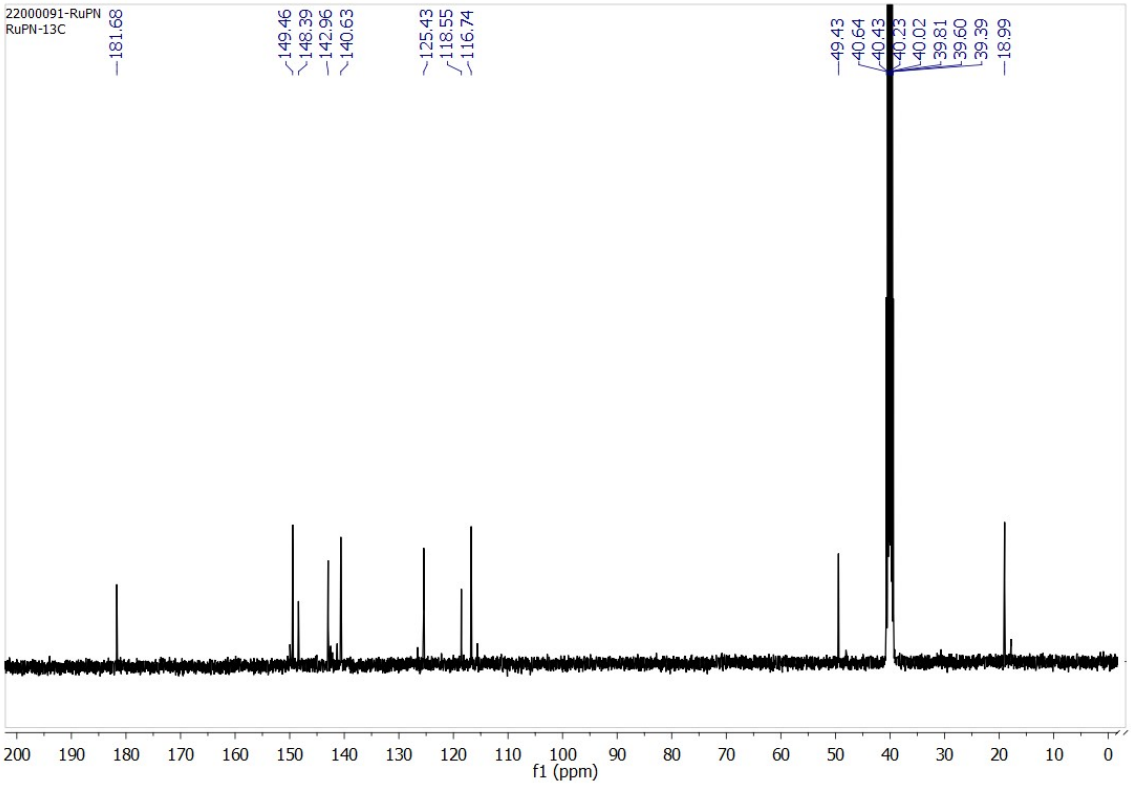

Figure SI9: ^{13}C−NMR spectrum of **6** in d_6-DMSO at room temperature.

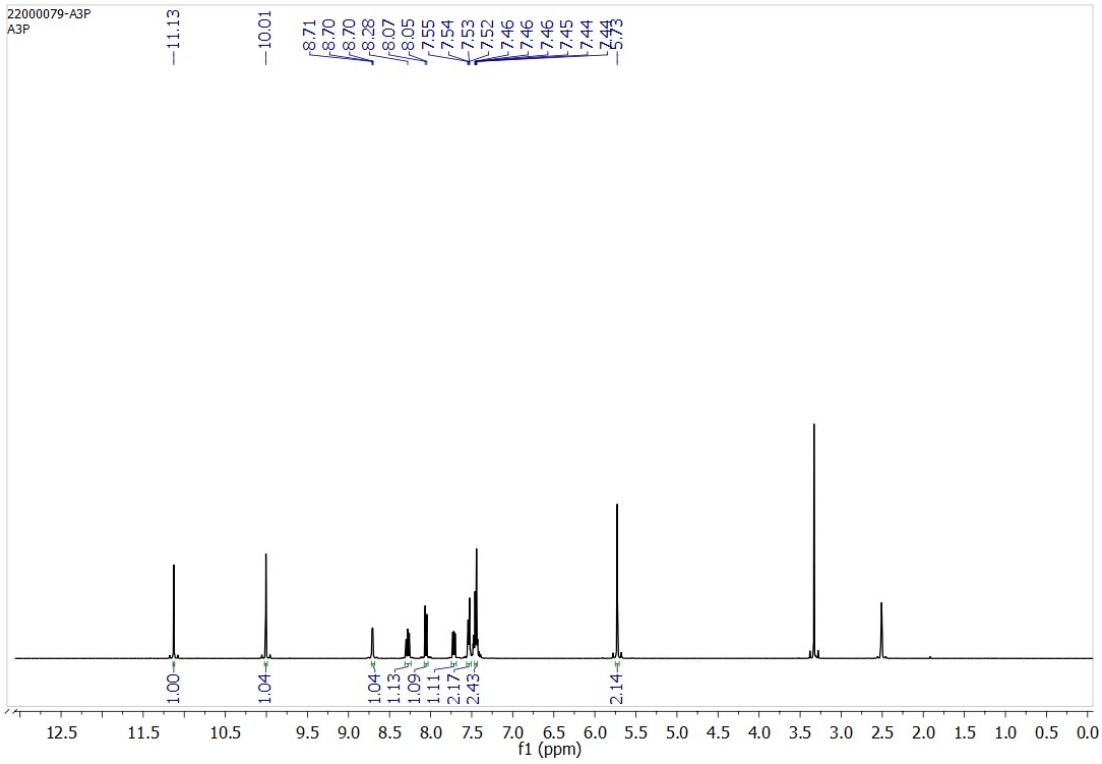

Figure SI10: ^{1}H−NMR spectrum of **5** in d_6-DMSO at room temperature.

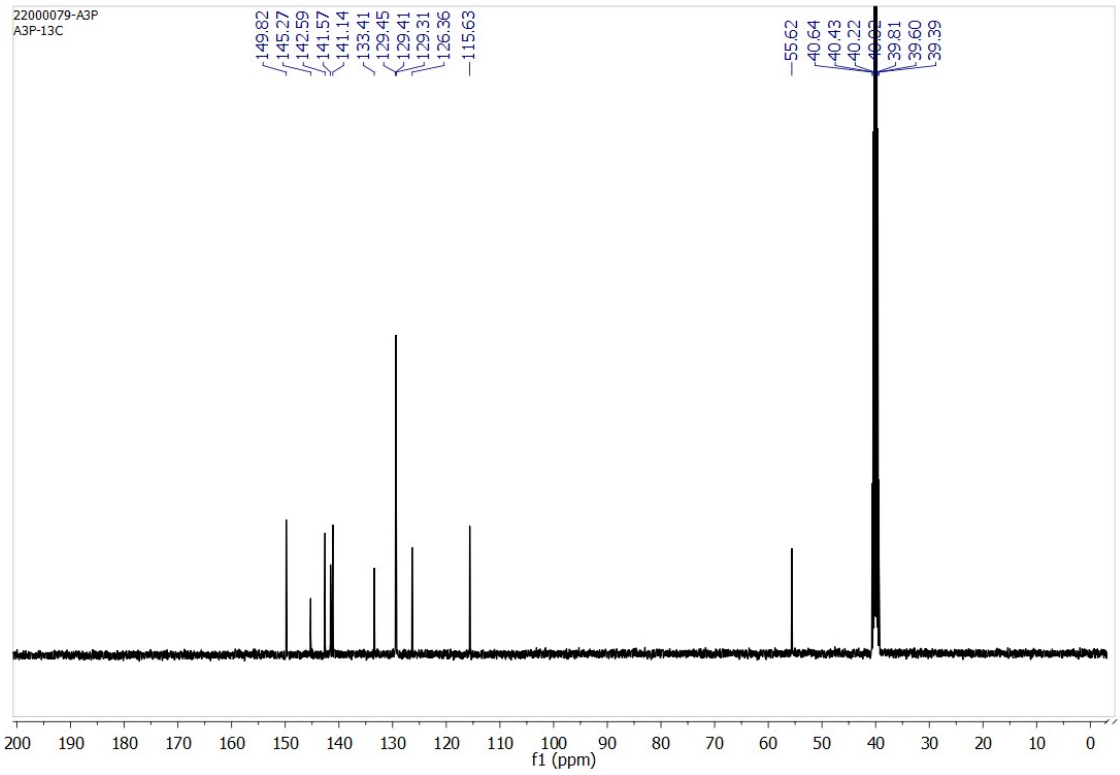

Figure SI11: ^{13}C−NMR spectrum of **5** in d_6-DMSO at room temperature.

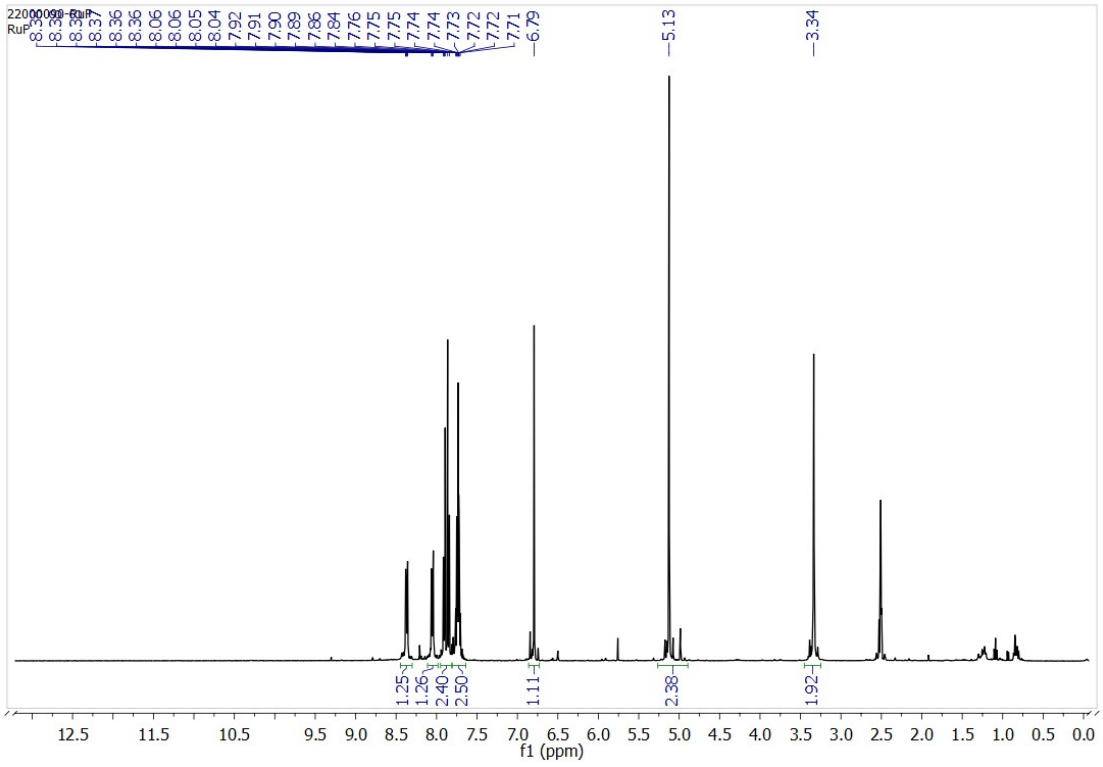

Figure SI12: ^{1}H−NMR spectrum of **7** in d_6-DMSO at room temperature.

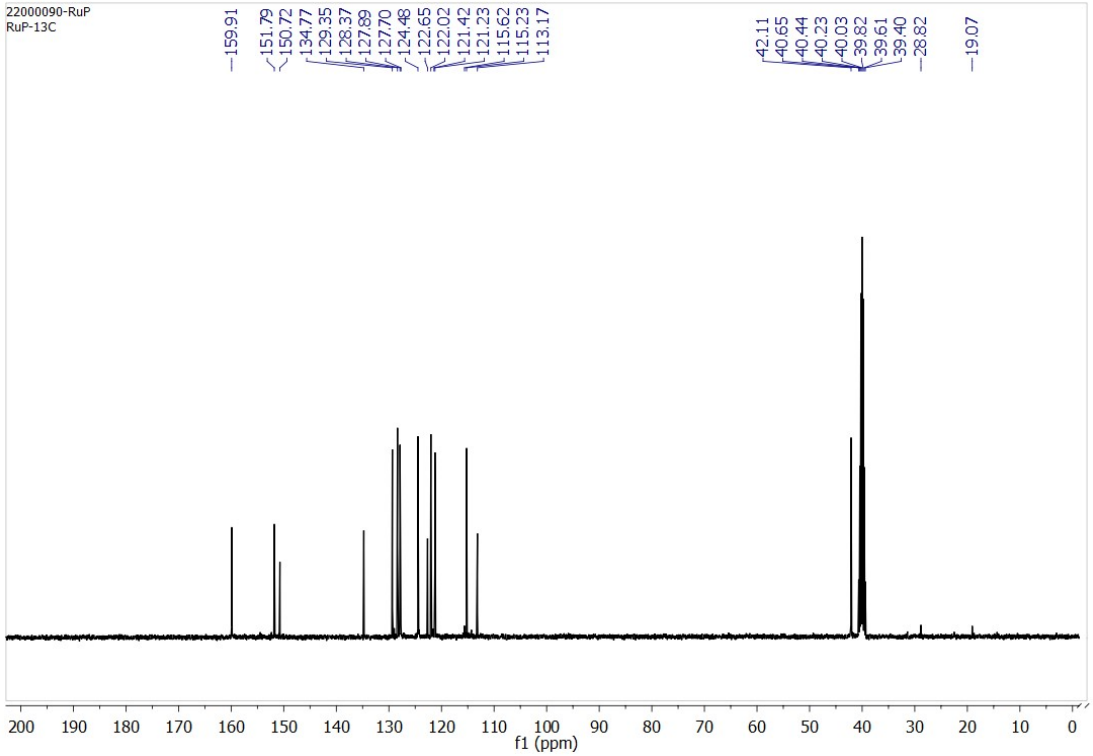

Figure SI13: ^{13}C−NMR spectrum of **7** in d_6-DMSO at room temperature.

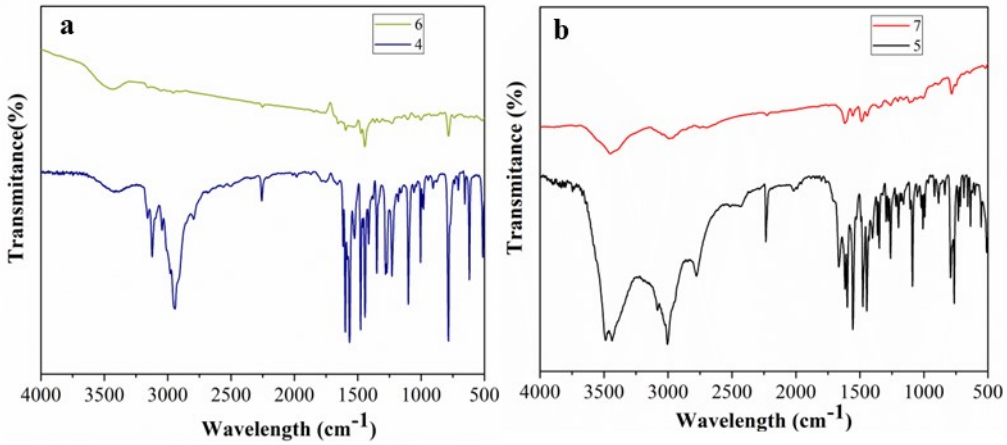

Figure SI14: IR spectra of salts **4** and **5** and their respective ruthenium organometallic polymers **6** and **7**.

Equation 1

Limit of detection (LOD)

LOD = 3*SD/S ; were SD is the standard deviation of blank and S is the slope of calibration curve.

Equation 2

Limit of quantification (LOQ)

LOQ = 10*SD/S; were SD is the standard deviation of blank and S is the slope of calibration curve.

Equation 3

Sensitivity = S/active surface area of working electrode; were S is the slope of the calibration curve.

References

[1] K. Fu, R. Zhang, J. He, H. Bai, and G. Zhang, "Sensitive detection of ketamine with an electrochemical sensor based on UV-induced polymerized molecularly imprinted membranes at graphene and MOFs modified electrode," Biosens. Bioelectron., vol. 143, no. May, p. 111636, 2019, doi: 10.1016/j.bios.2019.111636.

[2] Q. Li, W. Tang, Y. Wang, J. Di, J. Yang, and Y. Wu, "Electrochemiluminescence immunosensor for ketamine detection based on polyamidoamine-coated carbon dot

film," J. Solid State Electrochem., vol. 19, no. 10, pp. 2973–2980, 2015, doi: 10.1007/s10008-015-2913-9.

[3] Z. Bagheryan, J. B. Raoof, R. Ojani, and E. Hamidi-Asl, "Introduction of ketamine as a G-quadruplex-binding ligand using platinum nanoparticle modified carbon paste electrode," Electroanalysis, vol. 25, no. 12, pp. 2659–2667, 2013, doi: 10.1002/elan.201300418.

[4] K. Lian, P. Zhang, L. Niu, S. Liu, L. Jiang, and W. Kang, "A novel derivatization approach for determination of ketamine in urine and plasma by gas chromatography-mass spectrometry," J. Chromatogr. A, vol. 1264, pp. 104–109, 2012, doi: 10.1016/j.chroma.2012.09.058.

[5] R. A. Soomro, A. Nafady, K. R. Hallam, S. Jawaid, A. al Enizi, S. T. H. Sherazi, Sirajuddin, Z. H. Ibupoto, and M. Willander, "Highly sensitive determination of atropine using cobalt oxide nanostructures: Influence of functional groups on the signal sensitivity," Anal. Chim. Acta, vol. 948, pp. 30–39, 2016, doi: 10.1016/j.aca.2016.11.015.

[6] R. A. Dar, P. K. Brahman, S. Tiwari, and K. S. Pitre, "Electrochemical determination of atropine at multi-wall carbon nanotube electrode based on the enhancement effect of sodium dodecyl benzene sulfonate," Colloids Surfaces B Biointerfaces, vol. 91, no. 1, pp. 10–17, 2012, doi: 10.1016/j.colsurfb.2011.10.020.

[7] O. Ramdani, J. P. Metters, L. C. S. Figueiredo-Filho, O. Fatibello-Filho, and C. E. Banks, "Forensic electrochemistry: Sensing the molecule of murder atropine," Analyst, vol. 138, no. 4, pp. 1053–1059, 2013, doi: 10.1039/c2an36450f.

[8] A. F. João, R. G. Rocha, T. A. Matias, E. M. Richter, J. Flávio S. Petruci, and R. A. A. Muñoz, "3D-printing in forensic electrochemistry: Atropine determination in beverages using an additively manufactured graphene-polylactic acid electrode," Microchem. J., vol. 167, no. February, 2021, doi: 10.1016/j.microc.2021.106324.

[9] G. R. Fulmer, A. J. M. Miller, N. H. Sherden, H. E. Gottlieb, A. Nudelman, B. M. Bercaw, and K. Goldberg, "NMR chemical shifts of trace impurities: Common laboratory solvents, organics, and gases in deuterated solvents relevant to the organometallic chemist," Organometallics, vol. 29, no. 9, pp. 2176–2179, 2010, doi: 10.1021/om100106e.